Proceedings of the 1998 IEEE
International Conference on Robotics & Automation
Leuven, Belgium • May 1998

Transition Stability of Enveloped Objects

Makoto Kaneko, Mitsuru Higashimori, and Toshio Tsuji

Industrial and Systems Engineering
Hiroshima University
Kagamiyama Higashi-Hiroshima 739, Japan

Abstract

This paper discusses the transition stability in sliding an object enveloped by a multi-fingered robot hand whose joints are under constant torque command. We provide a new concept on transition stability, where a transition is called stable if the object is guaranteed to reach the goal section without moving away from a virtual cylinder defined in hand working space. To evaluate the transition stability, we introduce the force-flow-diagram enabling us to confirm whether the object moves to the designated direction or not. By using the diagram, we discuss the transition stability in lifting up an object to the palm under gravitational force. Simulation results show that the transition phase for a column object with concave surface is stable, while that having convex surface tends to be unstable. We also show experimental results to confirm the basic behaviours during the transition phase.

Key words: *Enveloping grasp, Grasp transition, Grasp stability, Constant torque control.*

1 Introduction

There have been a number of works concerning multi-fingered robot hand. Most of them address finger tip grasps. For this type of grasp, we can emphasize on dexterity and sensitivity. Enveloping grasp (or power grasp) provides another grasping style, where multiple contacts between one finger and the object are allowed. Such an enveloping grasp can support a large load in nature and is highly stable due to a large number of distributed contacts on the grasped object. While there are still many works in enveloping grasps, most of them discuss the contact force analysis [1]-[3], robustness of grasp [4], [5] and so forth, by implicitly assuming that the grasped object does not move.

On the other hand, we are particularly interested in the whole grasping procedure as shown in Fig.1, where the hand first approaches an object placed on a table (approach phase) and lifts up the object toward the palm (lifting phase) until an enveloping grasp (grasping phase) is completed [6]-[8]. In this paper, we focus on the final part of the lifting phase, where the object is still moving toward the palm. The motion planning of object in this phase can be regarded as an issue for manipulating an object enveloped by finger links. However, since contact forces can not be described explicitly, it is hard to determine the exact trajectory of object. In the lifting phase, fortunately, we do not care the exact trajectory of object, because the purpose is to simply move the object to the palm. We call such lifting phase transition phase as terminology. Can we always achieve a stable transition from an arbitrary point to the palm without dropping the object from hand under constant torque commands? This work is motivated by such a question.

We begin by defining a concept of transition stability in a general form. The basic idea of this definition is as follows. For example, let us consider a virtual pipe in the hand working space. If an object moves from one section to another without away from the surface of the pipe, we regard that the transition is stable in a global sense. This concept perfectly matches with the lifting phase since the goal is to convey the object to the palm without dropping the object from the hand. To utilize this concept, we introduce the *force-flow* which is a convenient tool for judging whether the object motion in the designated direction is realized or not. The *force-flow-diagram* is defined by the map displaying the *force-flow* at various position of the center of gravity of object. This diagram visually tells us a rough behaviour of object during a transition phase without solving any differential equations with respect to time. Additionally, this diagram provides us with an important information on the behaviour of object against a disturbance in the grasping phase. In conventional works, the robustness of enveloping grasps has been evaluated by the maximum external force and moment which can resist without sliding [1], [4] or by the volume of the convex polygon spanned by external force and moment that can resist without changing joint torques [5]. However, even though the object makes some slip due to an external disturbance, we can regard it stable in a global sense if the object comes back to the neighborhood of the original position after removing the disturbance, which is close to the stability concept based on the positive definiteness of stiffness matrix of the grasped object [9], [10]. We examine the transition stability for various objects by utilizing the *force-flow-diagram* introduced in this paper. Finally, we show a couple of experimental results to verify the transition stability in the vertical plane.

0-7803-4300-x-5/98 $10.00 © 1998 IEEE

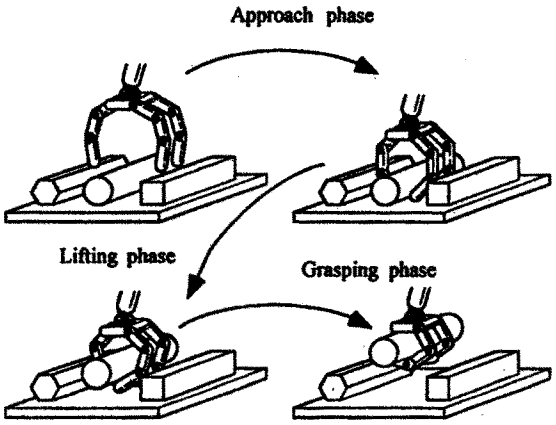

Fig.1 An example of enveloping grasp

2 Related Work

Approach phase:
Jeannerod[11] has studied human grasping intensively and has shown that during the approaching phase of grasping, the hand preshapes in order to prepare the shape matching with the object to be grasped. Bard and Troccaz[12] introduced such a preshaping motion into a robotic hand by utilizing low-level visual data.

Lifting phase:
Trinkle and Paul[13] proposed the concept of grasp liftability and derived the liftability regions of a frictionless planar object for use in manipulation planning.

Grasping phase:
Mirrza and Orin [1] applied a linear programming approach to formulate and solve the force distribution problem in power grasps, and showed a significant increase in the maximum weight handling capability for completely enveloping type power grasps. Trinkle [14] analyzed planning techniques for enveloping, and frictionless grasping. Salisbury [15] has proposed the Whole-Arm Manipulation (WAM) capable of treating a big and heavy object by using one arm which allows multiple contacts with an object. Bicchi [2] showed that internal forces in power grasps which allow inner link contacts can be decomposed into active and passive ones. Omata and Nagata [3] analyzed the indeterminate grasp force by considering that contact sliding directions are constrained in power grasps. Zhang et. al.[4] evaluated the robustness of power grasp by utilizing the virtual work rate for all virtual displacements.

Work combined with more than two phases:
Kleinmann et. al.[16] showed a couple of approaches for finally achieving a power grasp from a finger tip grasp. In our previous work [6], we have shown that human chooses the grasp planning according to the scale of objects, even though they are geometrically similar (Scale-Dependent Grasp). Based on the observation of human grasping, we introduced three grasping strategies depending upon the size of objects for cylindrical objects placed on a table [7],[8].

3 A Sufficient Condition for Moving an Enveloped Object

In this chapter, we first formulate the relationship between torque and contact force, and then consider a sufficient condition for moving an enveloped object.

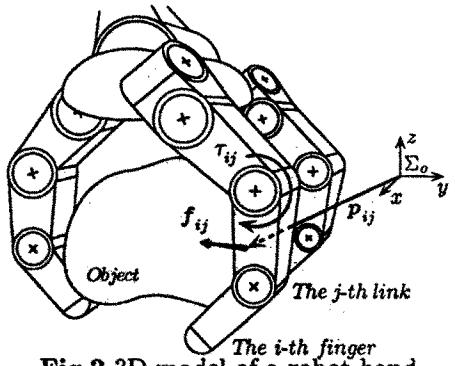

Fig.2 3D model of a robot hand

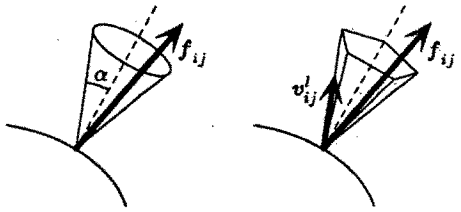

(a) friction cone (b) polyhedral convex cone

Fig.3 Friction cone and its model

3.1 Assumptions

To simplify the discussion, we set the following assumptions:

- Assumption 1: The robot finger has m fingers and n joints per finger.
- Assumption 2: The mass of finger link is negligible.
- Assumption 3: At each contact, we assume a Coulomb friction whose coefficient is given by μ, where both static and dynamic frictional coefficients are not distinguished.
- Assumption 4: Interference among fingers is ignored.
- Assumption 5: Each joint has a joint position sensor and a joint torque sensor.
- Assumption 6: Each link has at least one contact with the object.
- Assumption 7: The motion is slow enough to suppress any dynamic effect.

3.2 Relationship between torque and contact force

Let us consider the ith finger of the robot hand as shown in Fig.2. $\boldsymbol{p}_{ij} \in \mathcal{R}^{3\times1}$, $\boldsymbol{f}_{ij} \in \mathcal{R}^{3\times1}$ and $\boldsymbol{\tau}_i \in \mathcal{R}^{n\times1}$ denote the contact position vector, the contact force vector, and the joint torque vector, respectively, where i and j express the ith finger and the jth contact point, respectively.

Let $\boldsymbol{\tau}_i^j$ be the torque vector due to the contact force $\boldsymbol{f}_{i,j}$. $\boldsymbol{\tau}_i^j$ is given by

$$\boldsymbol{\tau}_i^j = \boldsymbol{J}_{ij}^{\mathrm{T}} \boldsymbol{f}_{ij} \tag{1}$$

where J_{ij}^T denotes the transpose of Jacobean matrix which maps the contact force into the joint torque. By utilizing the principle of superposition for the relationship between τ_i^j and f_{ij}, we can obtain

$$\tau_i = \sum_{j=1}^{k_i} \tau_i^j \quad (2)$$

$$= \sum_{j=1}^{k_i} J_{ij}^{\mathrm{T}} f_{ij} \quad (3)$$

where k_i denotes the number of the contact point of the ith finger. Eq.(3) is rewritten in the following form.

$$\tau_i = J_i^{\mathrm{T}} f_i \quad (4)$$

where

$$J_i^{\mathrm{T}} = \left[J_{i1}^{\mathrm{T}}, \ldots, J_{ik_i}^{\mathrm{T}}\right] \in \mathcal{R}^{n \times 3k_i} \quad (5)$$

$$f_i = \left[f_{i1}^T, \ldots, f_{ik_i}^T\right]^T \in \mathcal{R}^{3k_i \times 1} \quad (6)$$

Eq.(4) expresses the relationship between the contact force and the joint torque in ith finger. The contact force always appears within a friction cone as shown in Fig.3(a), where $\alpha = \tan^{-1}\mu$. In practice, the friction cone can be approximated by a polyhedral convex cone generated by a finite set of vectors (Fig.3(b)) such that we can obtain a set of linear equations [5]. Force set within the cone is represented by

$$f_{ij} = \sum_{l=1}^{L} \lambda_{ij}^l v_{ij}^l \qquad (\lambda_{ij}^l \geq 0) \quad (7)$$

where v_{ij}^l is the unit vector directing lth edge line. Note that in general the vectors v_{ij}^l are not linearly independent. Eq.(7) can be rewritten into the following form.

$$f_{ij} = V_{ij}\lambda_{ij} \quad (8)$$

where

$$V_{ij} = \left[v_{ij}^1, \ldots, v_{ij}^L\right] \in \mathcal{R}^{3 \times L} \quad (9)$$

$$\lambda_{ij} = \left[\lambda_{ij}^1, \ldots, \lambda_{ij}^L\right]^T \in \mathcal{R}^{L \times 1} \quad (10)$$

where L is the number of faces of polyhedral convex cone as shown in Fig.3(b). Applying eqs.(4) and (8) to m fingers, we obtain

$$\tau = J^{\mathrm{T}} f \quad (11)$$

$$f = V\lambda \quad (12)$$

$$\lambda \geq \mathbf{o} \quad (13)$$

where

$$\tau = \left[\tau_1^{\mathrm{T}}, \ldots, \tau_m^{\mathrm{T}}\right]^T \in \mathcal{R}^{mn \times 1} \quad (14)$$

$$J^{\mathrm{T}} = \begin{bmatrix} J_1^{\mathrm{T}} & & \\ & \ddots & \\ & & J_m^{\mathrm{T}} \end{bmatrix} \in \mathcal{R}^{nm \times 3\Sigma k_i} \quad (15)$$

$$f = \left[f_1^{\mathrm{T}}, \ldots, f_m^{\mathrm{T}}\right]^{\mathrm{T}} \in \mathcal{R}^{3\Sigma k_i \times 1} \quad (16)$$

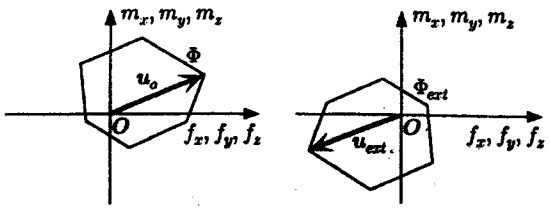

(a) Space $\Phi \ni O$ (b) External force space Φ_{ext}

Fig.4 Convex polygon spanned by Φ

$$V = \begin{bmatrix} V_1 & & \\ & \ddots & \\ & & V_m \end{bmatrix} \in \mathcal{R}^{3\Sigma k_i \times L\Sigma k_i} \quad (17)$$

$$V_i = \begin{bmatrix} V_{i1} & & \\ & \ddots & \\ & & V_{ik_i} \end{bmatrix} \in \mathcal{R}^{3k_i \times Lk_i} \quad (18)$$

$$\lambda = \left[\lambda_1^{\mathrm{T}}, \ldots, \lambda_m^{\mathrm{T}}\right]^{\mathrm{T}} \in \mathcal{R}^{L\Sigma k_i \times 1} \quad (19)$$

$$\lambda_i = \left[\lambda_{i1}^{\mathrm{T}}, \ldots, \lambda_{ik_i}^{\mathrm{T}}\right]^T \in \mathcal{R}^{Lk_i \times 1} \quad (20)$$

By deleting f from eqs.(11) and (12), we finally obtain

$$\tau = J^{\mathrm{T}} V \lambda \quad (21)$$

3.3 Basic behaviour under constant torque command

In both lifting and grasping phases, we apply constant torque command to each joint. Such a control scheme releases us from computing the exact contact forces as well as the exact object's position, since they are naturally determined by the combination among the command torque, the object's weight and the geometrical relationship. Under the constant torque control, eq.(21) results in mn equations for $L\Sigma_{i=1}^m k_i$ unknown variables λ. Generally, the number of unknown variables is greater than that of equations, and as a result, there exist infinite combinations of contact forces satisfying eq.(21) for a set of torque command. It is well known [5] that the resultant force f_o and moment m_o span a convex polygon Φ as shown in Fig.4(a), where u_o is a 6D vector given by

$$u_o = \begin{bmatrix} f_o \\ m_o \end{bmatrix} = \begin{bmatrix} \sum_{i=1}^{m}\sum_{j=1}^{k_i} f_{ij} + Mg \\ \sum_{i=1}^{m}\sum_{j=1}^{k_i} \{(p_{ij} - r_G) \times f_{ij}\} \end{bmatrix} \quad (22)$$

If Φ includes the origin O as shown in Fig.4(a), the commanded torque can generate at least one set of contact forces making $u_o = 0$, which means that the object will stop at the equilibrium point.

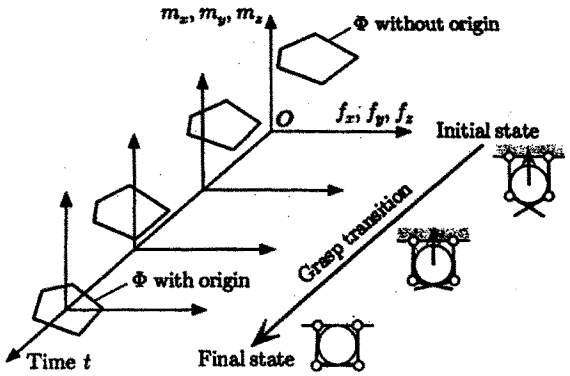

Fig.5 Grasp transition with Φ

3.4 A sufficient condition for moving an enveloped object

In our work, the torque command in the lifting phase should be determined, such that Φ may exclude the origin O as shown in Fig.5. Since Φ spans a convex polygon, the resultant force has the minimum and the maximum components for each axis. Therefore, by examining the maximum and the minimum values in a particular direction, we can evaluate whether the object moves in the direction or not. For example, if both have the positive signs in a particular direction, either a sliding or a rolling motion to the positive direction is guaranteed. As for a motion of enveloped object, the following theorem exists.

Theorem 1 *Consider ξ directional motion of object for a fixed center of gravity of object.*

(i) If $\{f_\xi^{min}\}^{min} \cdot \{f_\xi^{max}\}^{max} > 0$, it is guaranteed that the object moves to the $\mathrm{sgn}\left[\{f_\xi^{min}\}^{min}\right]$ *direction of ξ axis, where* $\mathrm{sgn}[v] = +1$ *for $v \geq 0$ and* $\mathrm{sgn}[v] = -1$ *for $v < 0$, and f_ξ^{min} and f_ξ^{max} denote the minimum and the maximum values in the ξ direction, respectively, and $\{\ \}^{min}$ and $\{\ \}^{max}$ denote the minimum and the maximum values for all possible orientations of the object, respectively. (A sufficient condition for moving an enveloped object in ξ direction)*

(ii) If $\{f_\xi^{min}\}^{min} \cdot \{f_\xi^{max}\}^{max} \leq 0$, the object motion in the specified direction is not uniquely determined.

Proof: Proof is straightforward. The motion of equation of the object is given by $M\ddot{\xi} = F_\xi$ where F_ξ denotes the force component in ξ direction. For example, $\{f_\xi^{min}\}^{min} > 0$ and $\{f_\xi^{max}\}^{max} > 0$ guarantee $F_\xi > 0$, which means that the object receives a positive acceleration by the contact forces and as a result, it moves to the positive direction of ξ axis, irrespective of orientation of object. Similarly, $\{f_\xi^{min}\}^{min} < 0$ and $\{f_\xi^{max}\}^{max} < 0$ guarantee $F_\xi < 0$, which means that the object receives a negative acceleration by the contact forces and, therefore, it moves to the negative direction of ξ axis. Then, we see the claim in (i) true. On the other hand, $\{f_\xi^{min}\}^{min} \leq 0$ and $\{f_\xi^{max}\}^{max} \geq 0$ mean that the object can stop if it is moving and it may not move if it is already stationary. Therefore, we can not clearly specify the motion in ξ axis. This leads to the claim in (ii). ■

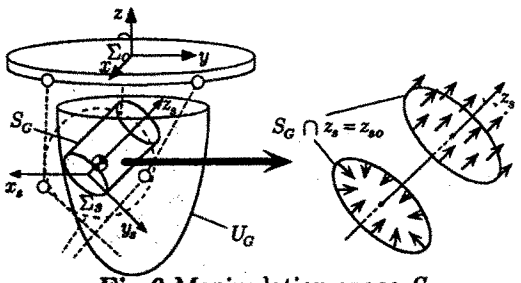

Fig.6 Manipulation space S_G

For example, let us regard ξ as the anti-gravitational direction. If $\{f_\xi^{min}\}^{min} > 0$ holds between the current position and the palm, the object moves upward until the motion is finally blocked by the palm. The moment the object motion is stopped by the palm, Φ includes the origin. Thus, the lifting phase is automatically switched into the grasping phase under object's constant torque control.

4 Transition Stability

Although the theorem 1 (i) ensures the object's motion in a particular direction, it does not specify anything on the object motion perpendicular to the particular direction. The object motions in the perpendicular directions are also important when discussing the behaviour of an enveloped object under constant torque control. For example, if the outward horizontal force is large enough during the lifting phase, the object will be away from the hand working space before reaching the palm. This is the reason why we need the discussion on the transition stability.

Let $p_G = (x_G, y_G, z_G)^{\mathrm{T}}$ be the gravitational center. To avoid multiple finger postures for a given gravitational center p_G, we assume that the swing d.o.f of each finger is fixed. Under this assumption, let us now define the transition stability following after an idea of virtual pipe.

Definition 1 *Let Σ_s be a coordinate system, where z_s axis is chosen such that it may coincide with the direction of the goal. Virtual pipe S_G is defined by (i) $S_G \subset U_G$ where U_G is the space spanned by p_G. (ii) S_G forms a cylindrical shape, where the section at $z_s = 0$ is the initial position of object and the other section is the goal.*

Definition 2 *The transition stability is guaranteed in S_G if the following two conditions hold in $z_{ss} \leq z_{so} \leq z_{sf}$, irrespective of the orientation of object.*

(i) For the circular cross section $z_s = z_{so}$, $\{(t^{\mathrm{T}} f_0)^{min}\}^{min} > 0$ for the positive goal $\{(t^{\mathrm{T}} f_0)^{max}\}^{max} < 0$ for the negative goal where t is the unit vector expressing the z_s axis.

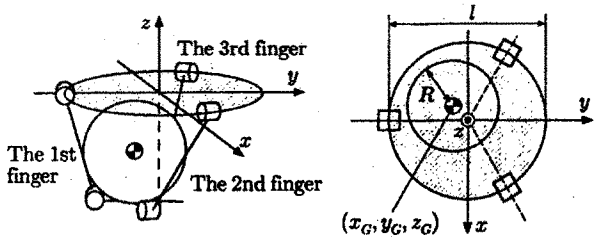

Fig.7 Simulation model for a sphere object

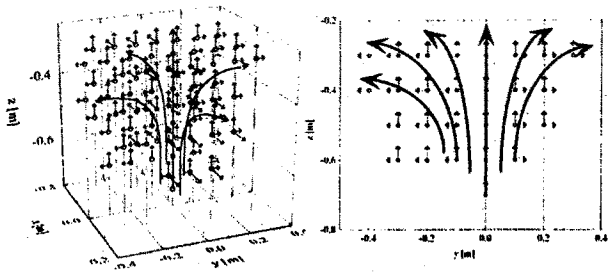

Fig.8 Force-flow-diagram for a sphere (l = 1.0[m], $R = 0.2$[m], $Mg = -1$[N] and $\alpha = \pi/18$[rad])

(ii) For the boundary of circular cross section $z_s = z_{so}$, $\{(n^{\mathrm{T}} f_0)^{max}\}^{max} > 0$ *and* $\{(n^{\mathrm{T}} f_0)^{min}\}^{min} > 0$ *where* $\boldsymbol{n}$ *is an inward normal unit vector at the boundary.*

In case that the goal is positive, the conditions (i) and (ii) in definition 2 are explained visually in Fig.6, where (i) is the sufficient condition for achieving the object's motion to the goal and (ii) is for keeping transition stability during the object's motion. While the definition 2 is a general definition on transition stability, we can easily apply it to the lifting phase in enveloping grasp by assigning the gravitational direction as z axis. Then, the goal is given by $z_{sf} = z_{spalm}$. If (i) and (ii) hold for $z_{ss} \leq z_{so} \leq z_{spalm}$, it is guaranteed that the hand lifts up the object to the palm without dropping the object from the hand, while the orientation of object is not specified.

5 Force-Flow-Diagram

In this section, we introduce the *force-flow-diagram* as a tool for judging whether the transition stability is confirmed under the torque command or not. We define a new coordinate system Σ_1 for *force-flow-diagram*. Based on theorem 1, we now define the *force-flow* and the *force-flow-diagram* as follows.

Definition 3 *Let* ξ *be either* x_1 *or* y_1 *or* z_1 *axis.*

(i) If $\{f_\xi^{min}\}^{min} \cdot \{f_\xi^{max}\}^{max} > 0$, *we put an arrow at* p_G *in* $\mathrm{sgn}\left[\{f_\xi^{min}\}^{min}\right]$ *direction in* ξ *axis.*

(ii) If $\{f_\xi^{min}\}^{min} \cdot \{f_\xi^{max}\}^{max} \leq 0$, *we put* $\circ$.

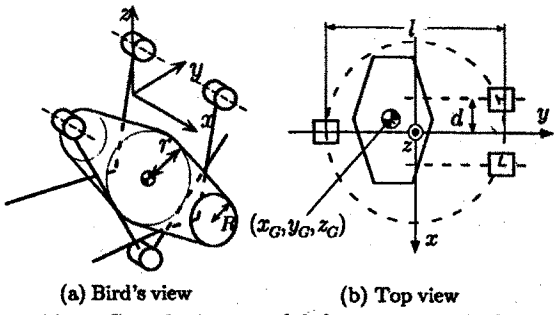

Fig.9 Simulation model for a tsuzumi object

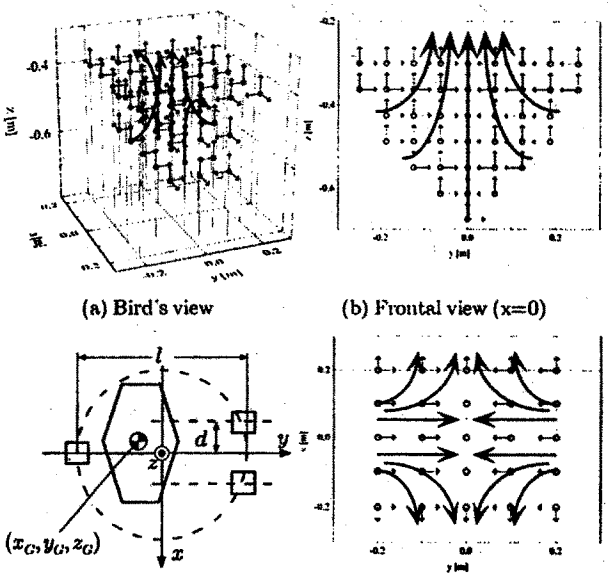

Fig.10 Force-flow-diagram for a sphere object (l = 1.0[m], d = 0.15[m], R = 0.2[m], r = 0.3[m] $Mg = -1$[N] and $\alpha = \pi/18$[rad])

We call the arrow or $\circ$ the *force-flow*. We also call the map displaying the *force-flow* at various position of the center of gravity of object the *force-flow-diagram*. A big advantage to utilize this diagram is that we can roughly estimate the object's behaviour without solving a set of differential equations with respect to time.

6 Simulations

6.1 Sphere object

A three fingered hand is assumed as shown in Fig.7, where each finger is fixed at the palm in every $2\pi/3$[rad]. Fig.8 shows the *force-flow-diagram* obtained by changing the center of gravity of the object, where $L = 15$, $R = 0.2$[m], and the first and the second torque commands are 2[Nm] and 1[Nm], respectively. An interesting observation in Fig.8 is that the object placed with a bit shift from z axis receives a force, such that it may always push the object away from the axis, which means that the object is easily dropped from the hand

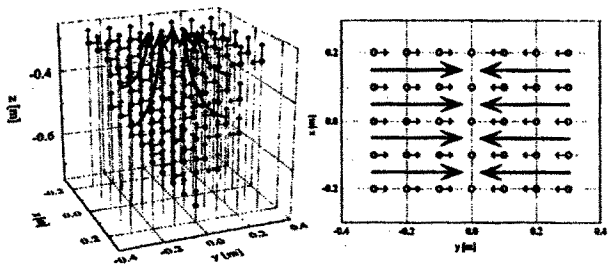

(a) Bird's view (b) Top view

Fig.11 Force-flow-diagram for $N = 40$, $l = 1.0$[m], $d = 0.15$[m], $R = 0.2$[m], $r = 0.2$[m] $Mg = -1$[N] and $\alpha = \pi/18$[rad]

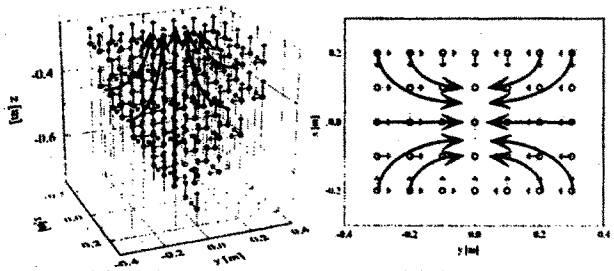

(a) Bird's view (b) Top view

Fig.12 Force-flow-diagram for $N = 40$, $l = 1.0$[m], $d = 0.15$[m], $R = 0.2$[m], $r = 0.1$[m] $Mg = -1$[N] and $\alpha = \pi/18$[rad]

during the lifting phase. Since S_G satisfying (ii) in transition stability can not be found in U_G, the transition stability is not guaranteed for a sphere.

6.2 Cylindrical objects

Three fingers are so arranged that the motion plane for each finger can be in parallel each other, as shown in Fig.9. In order to discuss the effect of curvature on the transition stability, we model the object characterized by two parameters, R and r. By setting $R < r$, and $R > r$, we can equivalently evaluate the effect of curvature on the transition stability. For $R = r$, the object's shape results in a cylinder. For $R > r$ and $R < r$, the surface becomes concave and convex, respectively.

Fig.10 shows the *force-flow-diagram* for $R < r$, where (a), (b), and (c) denote the bird's, the frontal and the top views, respectively. Fig.10(b) tells us that the object moves up stable in the frontal view, since we can easily find S_G satisfying (i) and (ii) in the transition stability, while S_G is not a 3D cylinder but a 2D rectangle in this case. However, Fig.10(c) shows an unstable behavior in the top view, where the object will easily move away from the working space, once the center of gravity shifts toward either the positive or the negative direction in x axis.

Fig.11 shows the top view of the *force-flow-diagram* for $R = r$ (cylindrical object). For such an object, it seems

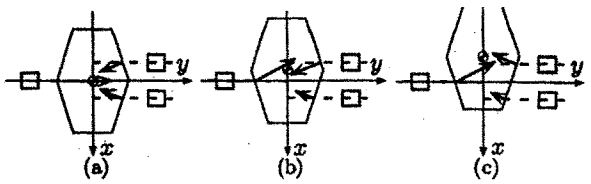

Fig.13 Qualitative explanation of contact force for a tsuzumi object ($R < r$)

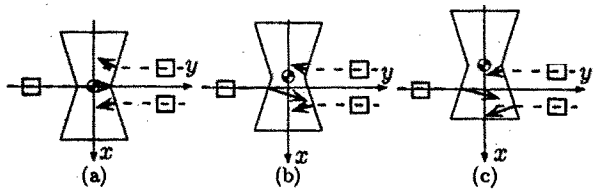

Fig.14 Qualitative explanation of contact force for a tsuzumi object ($R > r$)

to be a critical behavior, where we can not clearly specify whether the x-directional force results in either positive or negative.

Fig.12 shows the top view of the *force-flow-diagram* for $R > r$. For such an object, we can observe that the object whose center of gravity is placed in an arbitrary point always receives a force toward the origin of x, which is a stable behaviour. Totally judging, we have a tendency in which the lifting phase is achieved stably for a concave object, while it is unstable for a convex one.

Let us now explain why such behaviors are observed in the *force-flow-diagram*. Fig.13 and Fig.14 show qualitative explanation of contact forces for two different types of object, where Fig.13 and Fig.14 correspond to $R < r$ and $R > r$, respectively.

Suppose that we neglect the friction for simplifying the discussion. Also suppose that an object is shifted from the origin of x axis. Under frictionless contact, the contact force appears in the normal direction at the contact point. Therefore, we will have each contact force as shown in Fig.13 and Fig.14. These figures clearly tell us that the object receives a restoring force for $R > r$, while it receives a force making the system unstable for $R < r$.

7 Experiments

Fig.15 shows the behaviour of a cylindrical object after removing (a) vertical, and (b) 45 degrees-directional disturbances, respectively, where we attached a LED at the center of the object, so that we can observe the trajectory of the object after removing the disturbance. The experiment in Fig.15(a) is equivalent to the lifting phase under a gravitational force. Through these experiments, we can observe the stable behaviour in both lifting and grasping phases. This stability behaviour quite matches with the results obtained by simulations.

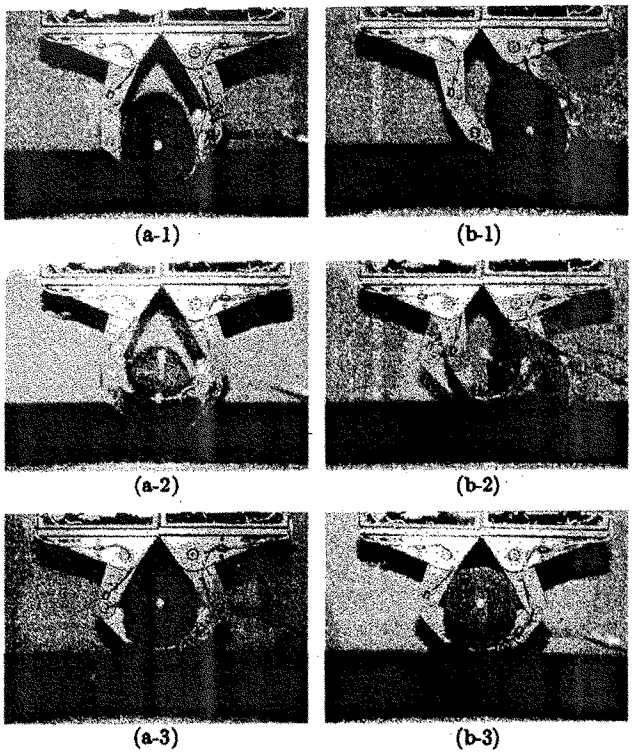

Fig.15 The behaviour of object after removing a disturbance

8 Conclusions

The main results obtained in this work are as follow:

(1) We showed a sufficient condition for sliding an object enveloped by a multi-fingered robot hand.
(2) We provided a general definition on the transition stability for an object enveloped by a multi-fingered robot hand.
(3) As a tool for evaluating the transition stability, we introduced the *force-flow-diagram*.
(4) Through simulations, we showed that the lifting phase in a column object is stable, while that having concave surface behaves unstable.
(5) For a column object, we experimentally confirmed the stable behaviours in the vertical plane.

This work was supported by the Inter University Robotics Project. Finally, I would like to express my sincere thanks to Mr. K. Furutera, Mr. N. Thaiprasert and Mr. Y. Hino for their cooperation in this work.

References

[1] Mirza, K. and D. E. Orin, "Control of force distribution for power grasp in the DIGITS system", *Proc. of the IEEE 29th CDC Conf.*, pp.1960–1965, 1990.

[2] Bicchi, A., "Force distribution in multiple whole-limb manipulation", *Proc. of the IEEE Int. Conf. on Robotics and Automation*, pp.196–201, 1993.

[3] Omata, T. and K. Nagata, "Rigid body analysis of the indeterminate grasp force in power grasps", *Proc. of the IEEE Int. Conf. on Robotics and Automation*, pp.1787–1794, 1996.

[4] Zhang, X-Y., Y. Nakamura, K. Goda and K. Yoshimoto, "Robustness of power grasp", *Proc. of the IEEE Int. Conf. on Robotics and Automation*, pp.2828–2835, 1994.

[5] Zhang, X. Y. Nakamura and K. Yoshimoto: "Mechanical Analysis of Grasps with Defective Contacts Using Polyhedral Convex Set Theory", *Journal of the Robotics Society of Japan*, Vol. 14, No. 1, pp. 105–113, 1996.(in Japanese)

[6] Kaneko, M., Y. Tanaka and T. Tsuji, "Scale-dependent grasp", *Proc. of the IEEE Int. Conf. on Robotics and Automation*, pp.2131–2136, 1996.

[7] M. Kaneko, Y. Hino, T. Tsuji: "On Three Phases for Achieving Enveloping Grasps", *Proc. of the 1997 IEEE Int. Conf. on Robotics and Automation*, 1997 (to appear).

[8] Kaneko. M, N. Thaiprasert, T. Tsuji: "Experimental approach on enveloping grasp for column objcts", *Preprints of 5th Int. Symp. on Exp. Robotics*, pp.17-29, 1997.

[9] Salisbury, J. K. : "Kinematics and force analysis of articulated hands", *Ph. D thesis, Dept. of Mechanical Eng. , Stanford Univ.*, 1982.

[10] Cutkosky, M. R., and I. Kao, : "Computing and controlling the compliance of a robotic hand", *IEEE Trans on Robotics and Automation, Vol.5, No.2.*, pp151-165, 1989.

[11] Jeannerod, M., "Attention and performance, chapter Intersegmental coordination during reaching at natural visual objects", pp.153–168, Erlbaum, Hillsdale, 1981.

[12] Bard, C. and J. Troccaz, "Automatic preshaping for a dexterous hand from a simple description of objects", *Proc. of the IEEE Int. Workshop on Intelligent Robots and Systems*, pp.865–872, 1990.

[13] Trinkle, J. C. and R. P. Paul, "The initial grasp liftability chart", *Trans. on Robotics and Automation*, Vol.5, No.1, pp.47–52, 1989.

[14] Trinkle, J. C., J. M. Abel and R. P. Paul, "Enveloping, frictionless planar grasping", *Proc. of the IEEE Int. Conf. on Robotics and Automation*, 1987.

[15] Salisbury, J. K., "Whole-Arm manipulation", *Proc. of the 4th Int. Symp. of Robotics Research*, Santa Cruz, CA, 1987. Published by the MIT Press, Cambridge MA.

[16] Kleinmann, K. P., J. Henning, C. Ruhm and H. Tolle, "Object manipulation by a multi-fingered gripper: On the transition from precision to power grasp", *Proc. of the IEEE Int. Conf. on Robotics and Automation*, pp.2761–2766, 1996.